Biochimica et Biophysica Acta, 1015 (1990) 69–78
Elsevier

BBABIO 43105

Conformational dynamic properties of water-soluble coupling factor of photophosphorylation studied by spin-labelling

Tsvetan Gantchev [1] Tsonka Tsanova [1], Georgi Gotchev [2] and Vladimir Timofeev [3]

[1] *Institute of Organic Chemistry, Bulgarian Academy of Sciences and* [2] *Sofia University, Faculty of Chemistry, Sofia (Bulgaria) and* [3] *Institute of Molecular Biology, Academy of Sciences USSR, Moscow (USSR)*

(Received 4 July 1989)

Key words: Coupling factor; Photophosphorylation; Spin labeling; ESR; CF_1; Conformational dynamics

The conformational dynamics of the isolated latent and activated water-soluble coupling factor of photo-phosphorylation (CF_1) was studied applying preferential spin-labelling of –SH, –COOH and $-NH_2$ amino acid side-chain groups and EPR spectra analysis permitting a quantitative discrimination between slow macromolecular rotation (τ_c) and fast anisotropic spin-label motion (S), as well as estimation of the relative distance between the nitroxide radicals attached to the protein. The labelling stoichiometry in most cases was found to depend on the enzyme activation state and medium pH. The protein correlation time (τ_c) of the non-activated CF_1 (tempoylmaleimide and tempoylisothiocyanate derivatives) was estimated to be 150–159 ns, and that of the activated CF_1 193–197 ns (data interpreted as CF_1 hydrodynamic volume enlargement after activation). The significant τ_c differences registered after ligation of the activated enzyme with ATP and Ca^{2+}-ATP are assigned to both segmental flexibility and hydration changes. The correlation time ($\tau_c = 10$ ns) obtained for tempoylcarbodiimide CF_1 derivative (probable labelling of β-subunit active site), together with the low spin-label restriction ($S = 0.78$) indicates a high degree of independent motion of the β-subunits with respect to that of the macromolecule, and/or microstructure flexibility in the vicinity of –COOH groups. When two carboxyl groups were modified (in the absence of Me^{2+} in the medium) the distance between the nitroxide radicals was calculated to be 45 Å, thus indicating that –COOH groups on different β-subunits were labelled. Conformational rearrangements (involving protein shadowing of several $-NH_2$ groups) were registered when the EPR spectra of latent and activated CF_1 tempoylisothiocyanate derivatives were analyzed by different techniques.

Introduction

Synthesis of ATP in green plants is mediated by the coupling factor. This enzyme consists of five distinct subunits, designated as α, β, γ, δ and ϵ, and is bound to the thylakoid membrane by its counter part (CF_0). It seems to be generally accepted that CF_1–CF_0 together function as a proton-translocating ATP-synthase utilizing energy derived from the transmembrane electrochemical gradient (reviewed in Ref. 1–3). The isolated CF_1 has a Ca^{2+}-dependent latent ATPase activity, which may be activated by trypsin or DTT-heat treatment [4]. The generation of electrochemical potential difference across the thylakoid membrane was shown to result in CF_1 conformational changes [5–7]. The ATPase activation of the isolated CF_1 also causes significant conformational changes as judged by the accessibility of inhibitors [8] and more recently by the introduction of various fluorescent [9,10], triplet [10,11] or spin labels [12]. The traditional versions of various physical labelling methods, when applied to studying the microstructure and microdynamics of macromolecules, however, have a number of inherent limitations (e.g., sensitivity to relatively high-correlation frequencies, high rate collision constants, etc.). Other limitations arise from the superimposition of both the slow macromolecular rotation in solution and the high-frequency motion of label molecules covalently bound within the protein. In our previous studies, we applied a new theoretical and experimental procedure, allowing to distinguish between the contribution of the slow protein rotation and fast

Abbreviations: CF_1, chloroplast coupling factor of photophosphorylation; TM, tempoylmaleimide spin label; TCC, tempoylcyclohexylcarbodiimide spin label; TITC, tempoylisothiocyanate spin label; DTT, dithiothreitol; FeCy, ferrycyanide; τ_c, protein rotational correlation time; S, effective order parameter; Mes, 4-morpholineethanesulfonic acid; Mops, 4-morpholinepropanesulfonic acid.

Correspondence: T. Gantchev, Institute of Organic Chemistry, Bulgarian Academy of Sciences, Acad. G. Bontchev Street, Building 9, 1140 Sofia, Bulgaria.

anisotropic motion of the covalently bound spin labels, to estimate macromolecular correlation times and/or local microstructure flexibility of various proteins [13–15]. In the present work this spin-label technique has been used to study the molecular dynamics properties of the water-soluble coupling factor (CF_1) in different activation states previously modified with spin labels at different positions (preferential labelling of –SH, –COOH and $-NH_2$ amino acid side chain groups). Additional information about protein subunit rearrangement after activation was obtained by estimating the relative distance changes between nitroxide radicals or by calculating the changes in their immersion depth with respect to the protein surface.

Materials and Methods

Materials. Tris, 2-amino-2-hydroxymethylpropane-1,3-diol; Mes and Mops buffers were obtained from Sigma. DTT and disodium EDTA were purchased from Serva. DEAE-Sephadex A-50, CL Sepharose-6B and Sephadex G-50 (fine) were Pharmacia Biotechnology Products. [γ-^{32}P] ATP was obtained from Amersham Corp. The spin labels: *N*-(1-oxyl-2,2,6,6-tetramethylpiperidinyl)maleimide (tempoylmaleimide, TM), 1-oxyl-2,2,6,6-tetramethyl-4-isothiocyanatopiperidine (tempoyl-isothiocyanate, TITC) and *N*-(1-oxyl-2,2,6,6-tetramethylpiperidinyl-4)-*N'*-(cyclohexyl)-carbodiimide (tempoylcyclohexylcarbodiimide, TCC) were synthesized according to the known procedures with slight modifications [16–18]. All other chemicals used were of reagent grade quality. Fresh commercial spinach for CF_1 isolation was supplied from a local plantation.

CF_1 purification. Chloroplasts were prepared from spinach leaves using standard methods [19]. Chloroform extraction of latent CF_1 was performed according to the method of Younis et al. [20]. The purification of the crude yellow-green extract on DEAE-Sephadex A-50 column was carried out as previously described [21] and the enzyme was precipitated in 50% ammonium sulphate and kept at 4°C. Before use the enzyme was desalted by centrifugation (18000 × *g* for 20 min), diluted with the desired buffer and further desalted by the centrifugation-chromatography procedure described by Penefsky [22]. According to polyacrylamide-sodium dodecylsulphate gel-electrophoresis the enzyme preparation was found to contain at least four types of subunits (α, β, γ and δ). Impurities detected were assigned to ribulose-bisphosphate carboxylase (8–12%). Therefore, before use the CF_1 preparations were passed through Sepharose 6B CL (2 × 120 cm column) in order to collect CF_1 fractions purified from ribulose-bisphosphate carboxylase.

CF_1 ATPase activity. The Ca^{2+}-dependent ATPase was activated prior to spin-labelling or after it, by heating CF_1 at 60°C for 4 min in: 40 mM ATP, 40 mM Mops (pH 8.0), 100 mM NaCl, 0.5–1.0 mM DTT and 2 mM EDTA. The DTT concentration was minimized, since it causes reduction of nitroxide radicals when heated (it was also noted that significant irreversible reduction of free radicals took place when the medium lacked (EDTA). The specific ATPase activity was assessed by the liberation of [^{32}P]P_i from [γ-^{32}P] ATP or by P_i colorimetric measurements. The reaction medium contained: 100 mM NaCl, 6 mM $CaCl_2$, 1 mM EDTA, 6 mM ATP, 40 mM Mops (pH 8.0) and 4–40 μg per ml CF_1, the incubation time was 10–30 min at 37°C. Protein concentration was determined according to the Bradford method [23]. The specific activity immediately after the activation of the unmodified CF_1 was 8–12 μmol P_i per mg protein per min.

Preparation of spin-label modified CF_1 derivatives. In the present work three different CF_1 derivatives were obtained, by preferential modification of –SH, $-NH_2$ and COOH protein amino acid side chain groups. Maleimide compounds are known to alkylate CF_1 sulfhydryl groups mainly on γ and ϵ subunits [9,23]. Modification of the accessible –SH groups on CF_1 was performed with tempoylmaleimide (TM). The reaction was allowed to proceed at ambient temperature (22°–23°C) for 6 h in 20 mM Mes (pH 6.6) or Mops (pH 8.0); 100 mM KCl; 1 mM ATP; 1 mM EDTA with 10-fold molar excess of the spin label. The protein concentration in aliquotes was 5–8 mg/ml. The reaction was terminated by double gel-filtration on Sephadex G-50 (fine) column applying the Penefsky method [22]. The molar ratios of bound spin-label molecules per CF_1 were calculated after double integration of the obtained EPR spectra, assuming CF_1 molecular weight of 405000 [25].

It has been reported earlier that carbodiimide compounds modify CF_1 –COOH groups at enzymatic sites responsible for Me^{2+} binding (most likely on β-subunit) [26,27]. The –COOH-modified CF_1 derivative was obtained incubating the protein with 10-fold molar excess of tempoyl-cyclohexyl carbodiimide (TCC) in a medium: 20 mM Mes (pH 6.2); 100 mM KCl; 1 mM EDTA, which contained or did not contain 40 mM $CaCl_2$. The unreacted spin-label molecules were removed as described above using an elution buffer: 20 mM Mops (pH 8.0); 100 mM KCl and 1 mM EDTA.

Fluorescent isothiocyanate reagents were reported to modify CF_1 $-NH_2$ groups [7,10,28]. It was suggested that the modified lysine group on the active site of the enzyme is essential for ATP binding and hydrolysis. Moreover, Wagner et al. [10,11] showed that CF_1 lysine groups were involved in subunit conformational rearrangement during ATPase activation. We performed also spin labelling of lysine residues of CF_1. For this purpose the purified nonactivated or activated CF_1 was treated with tempoyl isothiocyanate (TITC). The modification was performed varying TITC concentration in

a medium: 20 mM Mops (pH 8.0); 100 mM KCl; 1 mM ATP and 1 mM EDTA. The incubation time was 4 h at room temperature. CF_1 concentration was 5 mg/ml. The reaction was terminated as described above. The elution buffer contained 40 mM Mops (pH 8.0); 100 mM KCl; 1 mM ATP and 1 mM EDTA. The binding stoichiometries were determined as described below. In separate experiments, latent labelled CF_1 was subjected to DTT/heat treatment for 4 min.

EPR measurements and methods. EPR measurements were performed on Varian-E 104A or Bruker-ER 420 spectrometers equipped with variable temperature units, ER-4111 VT. In some experiments, the EPR spectrometer was connected by a CAMAC interface to a PDP 11 computer system to provide spectra accumulation, double integration, etc. Typical spectrometer settings (without microwave power saturation) were: microwave power of 6 mW, 9.76 GHz operating frequency, 1–2 G modulation amplitude at 100 kHz registration frequency (when only wide outer spectrum peaks were registered, the modulation amplitude used was 3.2 G). The measurements were performed at 20 °C. The accuracy of measuring the distance between outer wide peaks of the immobilized EPR spectrum ($2A'_{\parallel}$) was less than 0.1 G (when computer controlled). Continuous microwave saturation curves (at 77 K) were obtained on a Bruker-ER 420 spectrometer (klystron power of approx. 220 mW). EPR spectra simulation was performed by means of microcomputer adapted Freed's program [29] and the input dynamic parameters (τ_c and S) were estimated on the basis of the following considerations [14]:

It has been established that the distance between outer wide peaks of the EPR spectra of spin-labelled macromolecules ($2A'_{\parallel}$; Fig. 1) at normal conditions compared to their positions in the case of completely immobilized spins at 77 K ($2A_{zz}$) is determined by the degree of averaging of the nitroxyl radical hyperfine structure. It has been shown before [13] that the $2A'_{\parallel}$ changes can be presented as:

$$\Delta = 2A_{zz} - 2A'_{\parallel} = 2(A_{zz} - \bar{A}_{\parallel}) + 2(\bar{A}_{\parallel} - A'_{\parallel}) = \Delta_S + \Delta_\tau \quad (1)$$

where $2\bar{A}_{\parallel}$ is the distance between the outer wide peaks at infinite macromolecular correlation time ($\tau_c \to \infty$); Δ_S is the peak shift due to the fast anisotropic relative-to-protein motion of the spin label and Δ_τ is the shift due to the slow diffusional rotation of the macromolecule (see also Ref. 15). The computer simulation spectra analysis has shown that the second additive in Eqn. 1, Δ_τ, is in functional relation to τ_c and S ('order parameter') as follows:

$$\tau_c S = 197\left(\frac{\Delta_\tau}{S}\right)^{-1.39} \quad (2)$$

or

$$\Delta_\tau = C(S)\tau^{-\beta(S)} \quad (2')$$

where the correlation time (τ_c) is measured in nanoseconds and S is the quantitative parameter depending on the A and g tensors averaging due to the fast motion of the covalently bound to the protein spin label. According to the used dynamic model S is proportional to the orientational amplitude ('local protein flexibility') of the nirtoxide [14,30]:

$$S = \frac{\bar{A}_{\parallel} - a_0}{A_{zz} - a_0} \quad (3)$$

a_0 is the unbound nitroxyl isotropic hyperfine constant, equal to 17.1 G.

The experimentally determined dynamic parameters (τ_c and S), together with variations of some A and g tensor components, as well as the individual EPR line widths (W) were used to achieve optimal agreement between the experimental and model EPR spectra providing for a precise determination of the magnetic parameters determining the EPR spectrum specific shape features.

The information obtained by the estimation of the dynamic parameters (τ_c and S) of the spin-labelled CF_1 derivatives was further completed by several other EPR

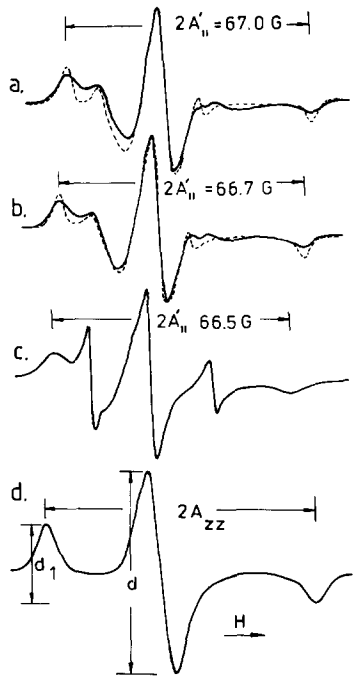

Fig. 1. EPR spectra of TM-CF_1 derivatives obtained at 20 °C and 0% sucrose (continuous lines): latent CF_1 labelled at pH 6.7 (a); activated CF_1 labelled at pH 6.7 (b) and pH 8.0 (c): typical spectrum obtained at 77 K and the parameter d_1/d used for calculation of the relative distance between the nitroxide radicals on CF_1 (d); computer-simulated EPR spectra (dashed lines) obtained using the experimental τ_c and S values (Table II) and hyperfine tensor components: $A_{xx} = 7.9$ G, $A_{yy} = 6.0$ G, $A_{zz} = 37.2$ G and $g = 2.0023$; g-factor anisotropy of 0.05, linewidth $W = 2.0$ G and nitroxide radical correlation time 0.2 ns.

techniques applied for determining of the relative distances of nitroxide radicals attached to the protein [31,32]. These techniques are based on the enhanced sensitivity of T_1 (spin-lattice relaxation) to the nitroxide environmental changes, when the rotation of the latter is hindered. In the present work, the relative distance between nitroxides covalently bound to CF_1 (in the absence of microwave power saturation) was determined according to the method of Kokorin et al. [31], using an appropriate calibration curve and measuring the d_1/d EPR spectrum parameter registered at 77 K (Fig. 1). The changes in the free radical immersion depth as related to the protein surface (TITC-CF_1 derivatives) were estimated monitoring the influence of the ferricyanide ions (FeCy), uniformly distributed in the aqueous phase on the continuous power saturation curves [32,33]. These experiments were performed in a glassy matrix (mixture buffer/sucrose, at 77 K). due to the system complexity (more than one label molecule per mol CF_1), the obtained results are mostly qualitative and represent the effective immersion changes of the spin-labels after the activation of the ATPase by DTT-heat treatment.

Results

Modification and rotational dynamics of tempoylmaleimide (TM) spin-labelled CF_1 derivatives

The reactivity of sulfhydryl groups on the different CF_1 subunits was shown to depend on the activation

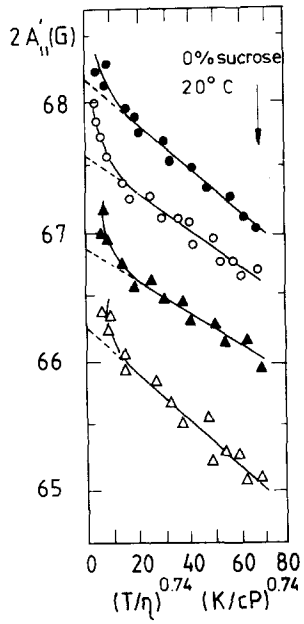

Fig. 2. Temperature/viscosity plots of $2A'_{II}$ vs. $(T/\eta)^{0.74}$ for TM-CF_1 derivatives: latent (●———●) and activated (○———○) enzymes labelled at pH 6.7; activated enzyme in the presence of 5 mM ATP (△———△) or 5 mM Ca^{2+}-ATP (▲———▲). The $2\bar{A}_{II}$ value is the linear extension intersection with the ordinate, $2A'_{II}$ value used is as indicated (at $T/\eta = 299$ K/cP).

TABLE I

The amounts of bound tempoylmaleimide (TM) spin label on the isolated CF_1, its Ca^{2+}-ATPase activity; EPR spectra parameters at 77 K (A_{zz} and d_1/d) and the calculated minimum distance (r) between the covalently bound TM molecules

Labelling conditions	TM/CF_1	Ca^{2+}-ATPase activity	A_{zz} (G) ±0.1	d_1/d	r ±2 (Å)
Latent (pH 6.7)	0.9±0.2	89 [a]	37.2	0.41	⩾ 50
Activated (pH 6.7)	2.3±0.2	63 [b]	36.9	0.52	35
Latent (pH 8.0)	4.6±0.6	75	36.6	0.54	32
Activated (pH 8.0)	8.3±1.0	37	36.1	0.61	28

[a] Percentage from unmodified latent enzyme activity (1 μmol inorganic phosphate per mg CF_1 per min).

[b] Percentage from unmodified activated enzyme activity (12 μmol inorganic phosphate per mg CF_1 per min).

state of the ATPase [9,24,34]. The labelling stoichiometry of the latent and activated CF_1 incubated with TM at different pH values, is shown in Table I. At pH 6.7, the TM/CF_1 molar ratio was found to be 0.9 ± 0.2 and 2.3 ± 0.2 for non-activated and activated prior to labelling CF_1, respectively. When labelling was done at pH 6.7 EPR spectra of completely immobilized labels were registered (FIg. 1a and b). If the alkylation reaction was carried out at pH 8.0, both strongly and weakly immobilized EPR spectrum components were observed (Fig. 1c). The total molar equivalents of TM incorporated in CF_1 were found to be 4.6 ± 0.6 (latent CF_1) and 8.3 ± 1.0 (activated CF_1). In the last case a strong inhibition of the labelled CF_1 ATPase activity was registered (Table I). The label distribution through CF_1 subunits was not studied. It can be expected that when CF_1 is labelled at pH 8.0, a partial modification of NH_2-side chain groups may also occur, too.

EPR spectra analysis shows that the A_{zz} spectrum parameter (obtained at 77 K) changes from 37.25 G (latent CF_1; pH 6.7) to 36.15 G (activated CF_1; pH 8.0), thus indicating that in all cases, when more than 1 mol TM per CF_1 is incorporated, spin-exchange interactions take place. On this basis, applying the method of Kokorin et al. [31], the relative distances between the nitroxide radicals, attached to CF_1, were determined measuring the d_1/d parameters of the spectra registered at 77 K (Fig. 1). The obtained r (Å) values (Table I) should be interpreted as minimum effective distances between the nitroxide radicals and only in the case of activated CF_1 (pH 6.7), where two nitroxide radicals are interacting, the r(Å) value should imply the correct distance between the former (35 Å).

The rotational dynamics of TM-CF_1 derivatives (latent and DTT-heat activated) labelled at pH 6.7 was studied by the method described in the Materials and

Methods. The quantitative analysis (τ_c and S estimation) was performed by recording EPR spectra at constant temperature (20°C) and varying medium viscosity. The obtained $2A'_{||}$ temperature/viscosity plots are shown are in Fig. 2. Each point in Fig. 2 is the average of 7–9 repeated independent measurements with $2A'_{||}$ values obtained after 5–7 computer-accumulated and averaged scans. The lines were plotted using the least-squares procedure. As can be seen from Fig. 2, the $2A'_{||}$ temperature/viscosity line slopes are small (Δ_τ is in the range of 1 G), which reflects high molecular mass of CF_1 and strong restriction of the spin-label motion. Experiments were carried out also in the presence of ATPase ligands (5 mM ATP and 5 mM ATP-Ca^{2+}). Using the plots from Fig. 2, the parameters necessary for τ_c and S calculation (Eqns. 2 and 3) were obtained (Table II). To verify the accuracy of the calculations a computer simulation was performed using the experimentally obtained τ_c and S values, together with appropriate values of non-axial g- and A-tensors and the individual linewidth (W) (see the legend of Fig. 1). The τ_c for latent and DTT-heat activated CF_1 are 150 ± 9 ns and 197 ± 16 ns, respectively, while the spin-label restriction is not significantly changed (S remains in the range 0.83–0.84), which corresponds to effective angular deviations of the spin-label in the range of 20–27° [30]. The correlation time τ_c in the absence of local (or segmental) flexibility of TM-CF_1 adduct is related to the volume of equivalent protein sphere: $\tau_c = \eta V_e / kT$ [35]. Thus, if CF_1 globule is approximated with a rigid sphere, hydrated volumes of $(6.2 \pm 0.6) \cdot 10^{-19}$ cm^3 and $(8.1 \pm 0.8) \cdot 10^{-19}$ cm^{-3} (radii of gyration, 54 ± 1 Å and 58 ± 2 Å) for latent and activated TM-CF_1 derivatives can be calculated (Table II) To ensure that the large volume increase after CF_1 activation is not due to aggregation effects (after DTT-heat treatment or TM-modification), the purified TM-CF_1 derivative was subjected to column chromatography on Sepharose 6B-CL (column 2×120 cm). The column was equilibrated with 20 mM Mops, 100 mM KCl and 1 mM EDTA (pH 8.0) and calibrated with spherical proteins of known molecular weight. The labelled CF_1 (latent and activated) was eluted in the same elution volume as the unlabelled one, appearing as a single peak with Stokes' radius of 55–60 Å.

Further results obtained in the presence of ATPase ligands also indicate changes in protein dynamics: 5 mM ATP (alone) leads to decrease both of the correlation time and the 'order parameter' ($\tau_c = 132 \pm 8$ ns; $S = 0.80 \pm 0.01$), while 5 mM ATP-Ca^{2+} induces a strong increase of τ_c to 220 ± 21 ns, accompanied by slight S change (Table II). The τ_c estimated after subsequent depletion of ligands, achieved by passing TM-CF_1 ATP (or ATP-Ca^{2+}) complex through Sephadex G-50 column, was found to be the same as for the activated enzyme in the absence of ligands (190–200 ns). It is, therefore, concluded that the significant τ_c changes in the presence of ATPase ligands are not due to experimental artifacts. Apparent decrease of CF_1 hydrodynamic volume in the presence of ATP was reported by Paradies [36], and assigned to decreased physical expansion of the molecule. However, in contrast to our results, studies performed by Kagawa and coworkers [37,38] on TF_1 (coupling factor isolated from thermophilic bacteria) indicated only subtle changes in protein radius of gyration upon nucleotide binding. It should be noted that a precise analysis of the nature of the changes in CF_1 dynamic parameters (τ_c and S) observed by the present spin-labelling technique, and a comparison of the results with those obtained by other techniques (on similar, but different objects) is hampered for several reasons, e.g., differences in the medium ionic strength, deviation from a spherical molecular shape, protein structure flexibility, etc. (see Discussion).

Tempoylcyclohexylcarbodiimide (TCC) modification of CF_1

Previous studies have shown that modification of CF_1-ATPase with carbodiimide derivatives (covalent labelling of –COOH groups at β-subunits) blocks catalytic and/or regulatory properties of the enzyme [26,27]. In the present work similar results were obtained when activated CF_1 was modified with TCC. The incubation of CF_1 with TCC was performed at pH 6.2 as described

TABLE II

EPR spectra parameters ($2\bar{A}_{||}$ and $2A'_{||}$) necessary for calculation of τ_c and S of TM-CF_1 derivatives (Eqns. 2 and 3); volume of equivalent sphere $V_e = \tau_c kT/\eta$ ($T/\eta = 299$ K/cP)

Averaged data ± standard deviation for 7–9 independent determinations.

TM-CF_1	$2A'_{||}$ (G)	$2\bar{A}_{||}$ (G)	Δ_τ (G)	S ±0.01	τ_c (ns)	V_e ($\times 10^{19}$ cm^3)
Latent	67.05	68.2	1.15	0.84	150± 9	6.2±0.6
Activated	66.65	67.6	0.95	0.83	197±16	8.1±0.8
Activated +5 mM ATP	65.05	66.3	1.25	0.80	132±8	5.5±0.4
Activated +5 mM Ca^{2+}-ATP	66.05	66.9	0.85	0.81	220±21	9.1±0.9

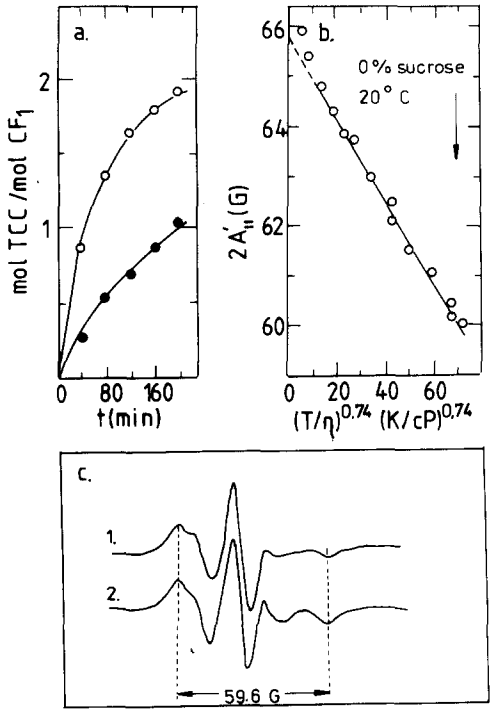

Fig. 3. The TCC-CF_1 derivatives: (a) TCC-labelling stoichiometry of the CF_1 without (○———○) or in the presence of divalent metal ions (●———●) in the reaction medium (40 mM $CaCl_2$); (b) $2A'_{||}$ temperature/viscosity plot obtained at 20 °C; and (c) experimental (1) and computer-simulated (2) spectra: Input parameters for simulation: $\tau_c = 10$ ns, $S = 0.78$, $A_{xx} = 7.8$ G, $A_{yy} = 7.8$ G, $A_{zz} = 37.2$ G, g-tensor assymetry of 0.05, linewidth 2.0 G and the nitroxide correlation time equals 0.1 ns.

in the Materials and Methods section. Fig. 3a shows the labelling stoichiometry in the presence or absence of divalent metal ions in the reaction medium. As can be seen from the figure, the presence of 40 mM $CaCl_2$ prevents modification of one of the two carboxyl groups and the resultant ATPase activity is about 75% from the original. The blocking of both accessible –COOH groups results in almost complete enzyme inactivation (92%).

The shape of the registered EPR spectra was independent of the labelling stoichiometry. The spectrum of TCC-modified CF_1 (two labels per mol CF_1) is shown in Fig. 3c. The spectrum is typical for moderately immobilized within the protein matrix spin-label (see below). The A_{zz} value (measured at 77 K) was equal to 36.85 G (weakly interacting spins) and the d_1/d value was found to be 0.42, which corresponds to a relative distance of 45 ± 3 Å between the two nitroxyl groups. These results are consistent with the assumption that the two modified carboxyl groups are located in different β-subunits of the enzyme. The dynamic equilibrium of the spin-labelled CF_1 was studied applying the same procedure as described for the TM-CF_1 derivative. The obtained $2A'_{||}$ temperature/viscosity plot is shown in Fig. 3b. When this plot is compared with the plots obtained for TM-CF_1 derivative (Fig. 2), a steeper line slope is obvious ($\Delta_\tau = 2\bar{A}_{||} - 2A'_{||}$, measured at 0% sucrose and 20 °C is equal to 5.9 G). The calculated τ_c and S values are equal to 10 ns and 0.78, respectively. These values, when put in a computer simulation program, give a spectrum shown in Fig. 3c, which seems to be a rather good approximation to the experimental one same $2A'_{||}$ value and overall shape). That is why the calculated τ_c and S values seem to be realistic and the fact that τ_c for TCC-CF_1 derivative is more than one order of magnitude lower than the obtained for TM-CF_1 derivatives is suggested to reflect the presence of high flexibility degree of the β-subunits as compared to the overall rotational dynamics of CF_1 (see Discussion).

Tempoylisothiocyanate (TITC) modification of CF_1

The stoichiometry of CF_1-TITC labelling and the Ca^{2+}-ATPase activity of the labelled enzyme as a function of TITC concentration for latent and previously activated CF_1 are shown in Table III. Obviously the protein conformational rearrangements during the activation process are accompanied by exposure of several new $-NH_2$ groups accessible for modification (the number of the extra sites at the saturation level is 3). It is also seen that the drop of ATPase activity is higher when DTT-heat 'opens' new accessible for modification NH_2 groups (most probably at the active site (s)).

The EPR spectra of the TITC-CF_1 derivatives show well distinguished immobilized and unimmobilized spectrum components (Fig. 4). The relative content of strongly (A) and weakly (B) immobilized spin-labels was different for the latent and activated enzymes (at the saturation level B/A is equal to 0.4 and 0.66, respectively). It is also notable that the $2A'_{||}$ values (at 0% sucrose and 20 °C, $T/\eta = 300$ K/cP) of the immobilized components are smaller than those obtained for TM – CF_1 derivatives (Figs. 1 and 4). However, the protein correlation times (τ_c, obtained after plotting the temperature/viscosity dependences of $2A'_{||}$ were found

TABLE III

The amounts of bound TITC spin label on latent and activated CF_1 and its Ca^{2+}-ATPase activity as a function of TITC concentration in the reaction medium

ATPase activity of the unmodified enzyme 0.9 μmol/P_i inorganic phosphate per mg CF_1min (latent) and 10 μmol inorganic phosphate per mg CF_1 min (activated).

TITC (μM)	TITC/CF_1		ATPase activity (%)	
	latent	activated	latent	activated
50	1.4	2.2	100	82
100	2.8	3.7	89	65
150	3.5	5.4	97	48
200	6.2	8.7	90	22
250	7.1	10.2	85	13
300	7.5	10.6	86	13

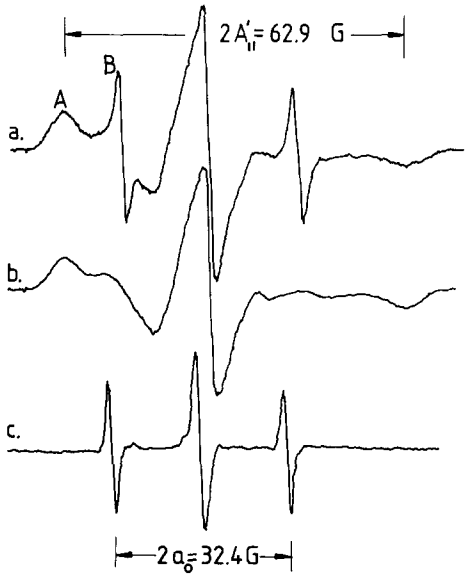

Fig. 4. (a) EPR spectrum on non-activated TITC-CF_1 derivative (7 mol TITC per mol CF_1), A and B are immobilized and mobile components, respectively; (b) spectrum obtained in the presence of 70 mM FeCy; and (c) derivative spectrum (mobile component in a pure form) obtained after computer substraction of spectrum (b) from spectrum a).

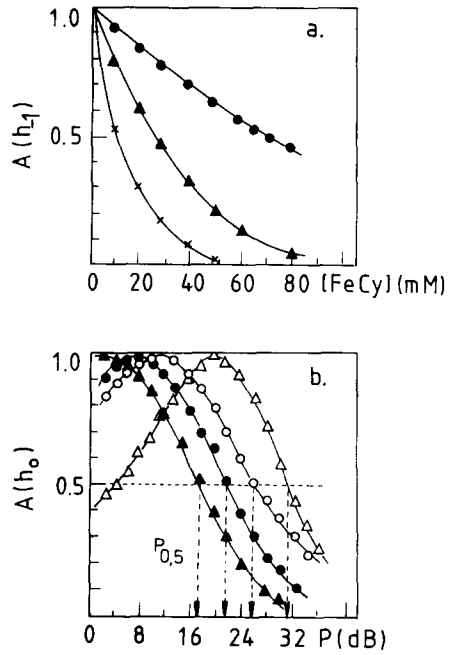

Fig. 5. The effect of FeCy on EPR amplitude of the high-field resonance line (h_{-1}) of spectrum component B (Fig. 4) at 20 °C (a); activated TITC-CF_1 derivative (●———●), latent TITC-CF_1 derivative (▲———▲) and free in the solution TITC spin label (×———×); and (b) the effect of FeCy on the microwave saturation curves (77 K) of TITC-CF_1 derivatives: latent (△———△) and activated (○———○) enzymes, without FeCy (open symbols), in the presence of 30 mM FeCy (closed symbols); $P_{0.5}$-values (dB) at 0.5 $A(h_0)_r$ indicative about the nitroxide spin-lattice relaxation rate changes.

to correspond to those obtained for TM-labelled CF_1 (Table IV).

The differences between latent and activated CF_1-TITC derivatives were further elucidated by monitoring the accessibility of paramagnetic ions (FeCy) to the bound nitroxides. The addition of 70–80 mM FeCy resulted in almost complete broadening of the unimmobilized component of the non-activated CF_1 (spectrum b in Fig. 4), while the same FeCy concentration was ineffective in broadening of the sharp spectrum component of the activated CF_1-TITC derivative (Fig. 5a). Probably after activation the protein matrix provides a barrier against the direct interaction of FeCy ions (from the bulk aqueous phase) with the relatively free tumbling nitroxides on CF_1. The computer substraction of spectrum 'b' from 'a' resulted in spectrum 'c' (mobile component in a pure form, Fig. 4). This procedure provided for estimation of the relative spin-label molar content (after double spectra integration) of both components (A and B) and for correlation time calculation of the mobile spectrum component. The results are summarized in Table IV. As can be seen, the amount of the mobile TITC labels doubles for the activated CF_1 and in the same time the correlation times and a_0 (the isotropic hyperfine constant) of the mobile component remain almost unaffected. It can be suggested that the activation of the Ca^{2+}-ATPase is accompanied by quaternary protein structural changes result-

TABLE IV

Dynamics parameters of TITC-CF_1 derivatives

Average ± standard deviations from nine independent determinations.

Enzyme	Immobilized component		Mobile component		mol mobile TITC
	protein correlation time τ_c (ns)	order parameter S ± 0.01	correlation time τ (ns) ± 0.1	a_0 (G) ± 0.1	mol total TITC
Latent	159 ± 10	0.78	0.5	16.2	$\frac{2}{7}$
Activated after labelling	193 ± 14	0.82	0.7	16.6	$\frac{4}{7}$

ing in exposure of several $-NH_2$ groups to an inner sequestered polar volume (the spin labels are freely tumbling, inaccessible for FeCy, and the a_0-value is typical for polar nitroxide environment).

Additional information about the enzyme conformational rearrangements after activation was obtained when latent CF_1-TITC derivative (7 mol TITC/mol CF_1) was exposed to DTT/heat treatment for 4 min. The EPR spectra analysis showed that the ratio of the mobile to the immobilized component (B/A) increases from 0.4 (latent) to 1.3 (activated CF_1). The relative increase of the mobile component (and the decrease of the immobilized one) was not due to hydrolysis of the bound label molecules during the DTT/heat treatment as checked by subsequent gel-filtration on Sephadex G 50 column. The differences in multisubunit structure between latent and activated after labelling CF_1 derivatives were further elucidated by registration of continous microwave saturation curves at 77 K in the absence or presence of rapidly relaxing paramagnetic ions (FeCy) in the surrounding medium (Fig. 5b). The $P_{0.5}$ values (shifts due to the interaction between FeCy and nitroxides on CF_1) are the quantitative parameters reflecting the increased spin-lattice relaxation and are determined by the minimum distance between a paramagnetic ion and the free radical centre. The obtained $P_{0.5}$ values, together with FeCy and nitroxide radical relaxation parameters, applied to the algorithm of Kulikov et al. [32,33] and assuming that the effective paramagnetic centre on CF_1 is located at a distance r (immersion depth) from the surface of a sphere with a radius $R = 60$ Å (CF_1 radius) and solvated FeCy ion radius of 18 Å, resulted in effective nitroxide immersion depth values of 8 Å and 19 Å for latent and activated enzymes, respectively. The calculated immersion depth change of 11 Å after activation (deeper buried nitroxides) is consistent with the results obtained by FeCy CF_1-TITC derivatives spectra titration at room temperature (Fig. 5a), and are indicative of the protein matrix shadowing of nitroxide radicals after CF_1 subunit structural rearrangements (probably involving the enzymatic active site (s)). However, due to the irregular nitroxide radicals distribution (weakly and strongly immobilized spins) within the protein, the calculated immersion change of 11 Å should be assumed to be a mean effective value.

Discussion

In the present work the dynamic properties of water-soluble coupling factor of photophosphorylation (CF_1) were studied applying spin-labelling and EPR spectra analysis, which allow qualitative estimation of nitroxide correlation times (at different degrees of spin-label immobilization) with an account to the relative nitroxide mobility, as well as estimation of nitroxides relative distance and immersion depth within the protein moiety. Based on the literature data, the different spin labels used in the present work are expected to react preferentially with –SH (TM, [24,34]), –COOH (TCC, [26,27]) and $-NH_2$ (TITC, [7,10,28]) CF_1 amino acid side chain groups. The estimated correlation times (τ_c) of different CF_1 spin-labelled derivatives, according to the present dynamic model, are expected to reflect the overall protein rotation (TM and TITC immobilized components), or the presence of high degree of protein segmental flexibility (TCC-adduct). The observed τ_c and S changes after enzyme activation may be attributed to protein conformational alterations (resulting in flexibility and/or hydration changes, see below). It is also suggested that the used spin-labels alkylate amino acid residues at or near to enzyme active or regulatory sites, since the ATPase activity of all spin-labelled derivatives studied is strongly inhibited.

The protein labelling with the sulfhydryl reagent (TM) at pH 6.7 resulted in modification of one –SH group (latent CF_1) and two SH-groups (activated CF_1). When the modification was performed at pH 8.0, a larger amount of bound spin-labels per mol CF_1 (latent and activated) was found. In all cases the modification of the activated enzyme led to considerable loss of ATPase activity. In several previous studies it has been shown that Cys 322 on γ-subunit is the residue which is modified by *N*-ethylmaleimide in the dark, while Cys 199–Cys 205 disulfide bond, which is reduced after DTT treatment, is essential for the regulation of the catalytic activity of CF_1 [34,39]. It is expected that one (or both) of the latter Cys residues are modified by TM after CF_1 activation. One disadvantage of the present study is that the exact location and distribution of TM among the protein –SH groups was not estimated at different labelling conditions. The measurement of A_{zz} EPR spectrum parameters (at 77 K) showed that, when more than 1 mol TM per mol CF_1 were bound, spin–spin interactions took place. This was attempted for estimation of the distances between TM spin-labels bound to different residues. Correct calculation of the nitroxide radical distance, however, could be made only for the activated CF_1 labelled at pH 6.7 (2 mol TM/CF_1). The obtained distance between the two labelled –SH groups is 35 Å, and hence it may be suggested that if only the γ-subunit is modified, the latter has a rather elongated form.

The rotational diffusion was estimated for latent and activated CF_1 (labelled at pH 6.7) and the results showed significant differences between the correlation times of both derivatives (Table II). It is also notable that the correlation times obtained for TM-CF_1 derivatives imply very low segmental flexibility (and existence of γ-subunit rigidly bound to the whole CF_1 globule). If CF_1 is approximated with a rigid hydrated sphere from the Perrin's formula ($\tau_c = \eta V_e/kT$) the following values

for CF_1 hydrated volumes can be calculated: $(6.2 \pm 0.6) \cdot 10^{-19}$ cm^3 (latent), $(8.1 \pm 0.8) \cdot 10^{-19}$ cm^3 (activated), $(5.5 \pm 0.4) \cdot 10^{-19}$ cm^3 (activated + ATP) and $(9.1 \pm 0.9) \cdot 10^{-19}$cm^3 (activated + Ca^{2+}-ATP) (Table II). These V_e values should be compared with the V_0 ones calculated according to Eqn. 4:

$$V_0 = \frac{M_r(v_h + \tilde{v})}{N_A} \quad (4)$$

where M_r is the molecular weight, v_h is the protein hydration in g H_2O per g protein, $\tilde{v}$ is the unhydrous specific protein volume and N_A is the Avogadro's number. For CF_1 molecular weight of 405 000 [25], partial anhydrous volume of 0.745 cm^3 and hydration level of 0.59 g H_2O per g CF_1 [40] have been determined before. These data substituted in Eqn. 4. give $V_0 = 9.0 \cdot 10^{-19}$ cm^3. This value (within the error margins) is close to experimentally obtained $V_e = (8.1 \pm 0.8) \cdot 10^{-19}$ cm^3 (activated CF_1) and $V_e = (9.1 \pm 0.9) \cdot 10^{-19}$ cm^3 (activated CF_1 + Ca^{2+}-ATP). In general, the difference between V_0 and V_e can be attributed to hydration changes and/or deviation of the molecular shape from spherical symmetry as well as, in the present case, to the existence of segmental protein flexibility in the region of the bound spin label [35]. The local flexibility (reflecting the spin label independent to the protein globule reorientational motion) is discriminated by separate estimation of τ_c and S. In their previous study Paradies et al. [40] have deduced that CF_1 particles are almost spherical with a radius of approx. 55.5 Å (latent enzyme). However, they have used an M_r value of 325 000–335 000, which results according to Eqn. 4. in $V_0 = 7.2 \cdot 10^{-19}$ cm^3 (whether the true molecular weight is 405 000 or 325 000, when loss of subunits is prevented, is under debate [2]). Therefore, an unequivocal interpretation of our results is not possible. We suggest that the changes of calculated τ_c (and V_e) values are mainly influenced by the changes of protein conformation (resulting in flexibility and/or hydration change). It is likely that an extensive hydration is the factor determining τ_c increase from 150 ns (latent TM-CF_1) to 197 ns (activated TM-CF_1). This assumption is based on previously reported data, indicating a presence of lower electron density CF_1 regions [40] and CF_1 conformational change after activation [10,11]. However, a possible contribution of 'tightening' effects (decreased segmental flexibility) cannot be ruled out. Again Paradies [36] has reported 'shrinkage' of CF_1 globule in the presence of nucleotides (ATP) and its dependence on the solution ionic strength. Previously, we also have observed changes of TM-CF_1 correlation time upon decrease of the ionic strength [12]. The obtained value of $\tau_c = 132$ ns ($V_e = (5.5 \pm 0.4) \cdot 10^{-19}$ cm^3) in the present study in the presence of ATP may reflect both decrease of CF_1 hydrodynamic radius and increased segmental flexibility of γ-subunit. The decrease of TM-spin label steric hindrance ($S = 0.80$, Table II) is also indicative of the increased segmental flexibility. It can be suggested that CF_1 conformation is stabilized (structure tightening) after complete ATPase ligation by Ca^{2+}-ATP. In this case the experimentally obtained $V_e = 9.1 \cdot 10^{-19}$ cm^3 is very close to that calculated from Eqn. 4 ($V_0 = 9.0 \cdot 10^{-19}$ cm^3). It is noteworthy that in their work Kinosita et al. [37], applying TF_1 labelling with fluorescent dye *N*-(1-pyrene)maleimide and measuring the fluorescence anisotropy decay, were able to detect only subtle TF_1 conformational changes on nucleotide binding. Unfortunately, in this paper τ_c values obtained at 20 °C are not reported, but only the values measured at 5 °C ($\tau_c = 160$ ns) and at 45 °C ($\tau_c = 120$ ns). Linear extrapolation of these data will give $\tau_c \approx 140$–145 ns at 20 °C, which is in the range of τ_c values obtained in the present study for latent CF_1 and activated CF_1(+ATP). However, when compared the fluorescence decay data with those obtained in the present study, it should be enphasized that: (i) the steric hindrance (and its change) of the fluorescent label cannot be easily discriminated from the direct anisotropy decay measurements; (ii) the ionic strength of the solution in the experiments performed by Kinosita et al. is rather low; and (iii) it is doubtful whether TF_1 and CF_1 dynamic properties in solution are close enough, since X-ray scattering experiments performed by Furuno et al. [38] on TF_1 indicated rather ellipsoidal shape of the protein, contrary to the observations of Paradies et al. [40] which have concluded from similar measurements that CF_1 particles are almost spherical.

One attractive explanation of the increased CF_1 hydration volume (especially after activation) may be the hypothesis of the sequestered solvated space in its globule [41]. The results obtained in the present work with the TITC-CF_1 derivative are also in confirmation of such an assumption. We have found that when labelled CF_1 is activated, two $-NH_2$ groups (probably at the active site) are transferred from protein environment, where they are strongly immobilized to loci, where the latter are freely tumbling. Moreover, after activation the $-NH_2$ groups become unaccessible to the spin-broadening agent (FeCy), uniformly distributed in the surrounding medium. On these grounds and accounting for the fact that the a_0-value of the unimmobilized EPR-spectrum component remains relatively high, it can be concluded that at least part of the free tumbling spin-labels (their total number is 4) occupy some closed inner aqueous volume. It is noteworthy that the calculated rotational correlation time of TITC-CF_1 derivative (193 ns, for the immobilized component) almost coincides with that obtained for TM-CF_1 derivative in similar conditions (197 ns). Thus the strongly restricted motion of TM and TITC spin-label molecules (S = 0.84–0.90) reflect the overall CF_1 macromolecular rota-

tion in solution. On the contrary, the dynamic parameters of TCC-CF_1 derivative (τ_c and S) were found to decline significantly as compared to the TM-CF_1 and TITC-CF_1 ones. The measured distance between the two labelled groups (most likely –COOH groups on β-subunits) is more than 46 Å. This implies that two different β-subunits of the enzyme are labelled, since this distance is larger than the expected diameter of a globule with 54000–58000 Da (the molecular mass of α and β subunits). The results showing that one of the COOH groups can be prevented from modification with the TCC reagent by divalent metal ions should imply also that both –COOH groups are not in equivalent states. However, the estimated dynamics parameters ($\tau_c = 10$ ns and $S = 0.78$) were independent of the labelling stoichiometry. As in the case of TITC-CF_1 derivatives (presence of relatively weakly immobilized spin-label component in the active site) TCC-derivatives also show very low value of τ_c as compared to the overall CF_1 dynamics (e.g., TM-derivative). We suggest that the observed fast relaxation time of TCC labels attached to –COOH CF_1 groups is consistent with any of the possibilities: (i) the β-subunit region in the vicinity of the labelled –COOH group undergoes extensive segmental fluctuations (structure flexibility) and/or (ii) the β-subunit globule is able to have a high degree of rotational freedom independent of the whole CF_1-globule. The local flexibility of α-subunit, which has a similar molecular mass to the β-subunit and is also involved in CF_1 catalytic activity, has been reported previously [42]. The similar dynamic properties of α and β subunits (high dynamic flexibility and/or independent rotation) may account for some important catalytic properties of theirs, as it was suggested earlier in the CF_1 nucleotide exchange functional model of Kozlov [43].

Acknowledgement

One of the authors (Ts.G.) would like to thank Prof. I.A. Kozlov and Dr. A.N. Malyan for the helpful discussions.

References

1 Nelson, N. (1977) Biochim. Biophys. Acta 456, 314–338.
2 Kagawa, Y., Sone, N., Hirata, H. and Yosida, M. (1979) J. Bioenerg. Biomembr. 11, 39–77.
3 Cross, R.L. (1981) Annu. Rev. Biochem. 50, 681–714.
4 Vambutas, V.K. and Racker, E. (1965) J. Biol. Chem. 240, 260–266.
5 Weiss, M.A. and McCarty, R.E. (1977) J. Biol. Chem. 246, 8007–8012.
6 Kraayenhof, R. (1977) in: Current topics in bioenergetics (Rao Sanidi, D., ed.), pp. 423–428. Academic Press, New York.
7 Wagner, R. and Junge, W. (1980) FEBS Lett. 114, 327–333.
8 Vallejos, R.H., Ravizzini, R.A. and Andreo, C.S. (1977) Biochim. Biophys. Acta 459, 20–26.
9 Holowka, D.A. and Hammes, G.G. (1977) Biochemistry 16, 5538–5545.
10 Wagner, R., Carrillo, N., Junge, W. and Vellejos, R.H. (1981) FEBS Lett. 136, 208–212.
11 Wagner, R. and Junge W. (1982) Biochemistry 21, 1890–1899.
12 Gantchev, Ts., Mominov, P.T., Verchoturov, V.N., Timofeev, K.N. and Timofeev, V.P. (1987) Molek. Biol. USSR 21, 1033–1038.
13 Timofeev, V.P. and Tsetlin, V.I. (1983) Biophys. Struct. Mech. 10, 93–108.
14 Timofeev, V.P. (1986) Molek. Biol. USSR 20, 697–711.
15 Gantchev, Ts., Costadinova, Zl. and Ganeva, E. (1988) Biochim. Biophys. Acta 953, 218–225.
16 Griffith, O.H. and McConnell, H.M. (1966) Proc. Natl. Acad. Sci. USA 56, 809–813.
17 Stone, T.J., Buckman, T., Nordio, P.L. and McConnell, H.M. (1965) 54, 1010–1017.
18 Kumaraev, V.P. and Knorre, D.G. (1970) Dokl. Akad. Nauk SSSR 193, 103–105.
19 Winget, G.D., Izawa, N. and Good, N.E. (1965) Biochem. Biophys. Res. Commun. 21, 438–443.
20 Younis, H.M., Winget, G.D. and Racker, E. (1977) J. Biol. Chem. 252, 1814–1818.
21 Lein, S. and Racker, E. (1971) Method Enzymol. 547–555.
22 Penefsky, H.S. (1977) J. Biol. Chem. 252, 2891–2899.
23 Bradford, M.M. (1976) Annal. Biochem. 72, 248–254.
24 McCarty, R.E. and Fagan, J. (1973) Biochemistry 12, 1503–1507.
25 Moroney, J.V., Lopesti, L., McEwen, B.F., McCarty, R.E. and Hammes, G.G. (1983) FEBS Lett. 158, 58–62.
26 Arana, J.L. and Vellejos, R.H. (1981) FEBS Lett. 123, 103–106.
27 Malyan, A.N., Zakharov, S.D. and Proskuryakov, I.I. (1981) Biochem. Physiol. Pflanzen 176, 828–834.
28 Pick, U. (1981) Biochem. Biophys. Res. Commun. 102, 165–171.
29 Freed, J. (1979) in Spin Labeling, Theory and Applications, (Berliner, L., ed.), pp. 137–1153, Mir Publications, Moscow.
30 Griffith, O.H. and Jost, P. (1979) in Spin Labeling, Theory and Applications (Berliner, L., ed.), pp. 489–569, Mir Publications, Moscow.
31 Kokorin, A.I., Zamaraev, K.N., Grigorijan, G.L., Ivanov, V.P. and Rozantsev, E.G. (1972) Biofizika USSR 17, 34–41.
32 Kulikov, A.V., Cherepanova, E.S. and Bogatyrenko, V.R. (1981) Theor. Exp. Chem. USSR 17, 788–797.
33 Likhtenstein, G.I., Kulikov, A.V., Kotelnikov, A.I. and Levchenko, L.A. (1986) J. Biochem. Biophys. Methods 12, 1–28.
34 Moroney, J.V., Fullmer, C.S. and McCarty, R.E. (1984) J. Biol. Chem. 259, 7281–7285.
35 Yguerabide, J. (1972) Methods Enzymol. 23, 498–578.
36 Paradies, H.H. (1980) Biochem. Biophys. Res. Commun. 96, 1357–1363.
37 Kinosita, K., Ikegami, A., Yoshida, M. and Kagawa, Y. (1982) J. Biochem. 92, 2043–2046.
38 Furuno, T., Ikegami, A., Kihara, H., Yoshida, M. and Kagawa, Y. (1983) J. Mol. Biol. 170, 137–153.
39 Miki, J., Maeda, M., Mukohata, Y. and Futai, M. (1988) FEBS Lett. 232, 221–226.
40 Paradies, H.H., Zimmermann, J. and Schmidt, V.D. (1978) J. Biol. Chem. 253, 8872–8879.
41 Wagner, R., Andreo, C. and Junge, W. (1983) Biochim. Biophys. Acta 723, 123–127.
42 Paradies, H.H. and Kagawa, Y. (1981) FEBS Lett. 136, 3–7.
43 Skulachev, V.P. and Kozlov, I.A. (1977) The Proton Adenosinetriphosphatases (Jasaitis, A.A., ed.), Nauka, Moscow.